Experimental characterization of a bi-dimensional array of negative capacitance piezo-patches for vibroacoustic control

F.Tateo[a], M. Collet[a], M. Ouisse[a], M.N. Ichchou[b] and K.A. Cunefare[c]

[a]Femto-st, 24 rue de l'Epitaphe, Besancon, France
[a]LTDS, 36 avenue Guy de Callongue, Lyon, France
[b]G.W. Woodruff School of Mechanical Engineering, 113 Erskine Love Building, Atlanta, GA

ABSTRACT

A recent technological revolution in the fields of integrated MEMS has finally rendered possible the mechanical integration of active smart materials, electronics and power supply systems for the next generation of smart composite structures. Using a bi-dimensional array of electromechanical transducers, composed by piezo-patches connected to a synthetic negative capacitance, it is possible to modify the dynamics of the underlying structure. In this study, we present an application of the Floquet-Bloch theorem for vibroacoustic power flow optimization, by means of distributed shunted piezoelectric material. In the context of periodically distributed damped 2D mechanical systems, this numerical approach allows one to compute the multi-modal waves dispersion curves into the entire first Brillouin zone. This approach also permits optimization of the piezoelectric shunting electrical impedance, which controls energy diffusion into the proposed semi-active distributed set of cells. Furthermore, we present experimental evidence that proves the effectiveness of the proposed control method. The experiment requires a rectangular metallic plate equipped with seventy-five piezo-patches, controlled independently by electronic circuits. More specifically, the out-of-plane displacements and the averaged kinetic energy of the controlled plate are compared in two different cases (open-circuit and controlled circuit). The resulting data clearly show how this proposed technique is able to damp and selectively reflect the incident waves.

Keywords: negative capacitance, smart materials, metacomposite, Bloch theorem, experiment.

1. INTRODUCTION

The design of innovative structures having new physical functionalities represents a big challenge for both industrial and academic communities. In the vibration domain a very important issue is the capacity of controlling the dynamic behavior of a structure by acting on the mechanical power flow in terms of transmitting and absorbing properties. Among all proposed solutions, distributed control system integrating shunted piezoelectric patches represents an interesting solution[9] . Different circuit's layouts can be considered, for example a control strategy based on resonant circuit where the modification of the external circuit's parameters allows the suppression of a resonant peak.[8] A different approach based on negative capacitance circuit allows a widening of the control frequency band. In order to magnify this effect a lattice of actuators connected to the circuits is introduced. Up to now this technique has been mainly applied to mono-dimensional structures such bars and beams[1] or bi-dimensional structures such plates and shells.[3] The aforementioned works are characterized by the presence of multiple actuators placed over the entire surface of the controlled structure. In this work the previous idea is modified introducing the concept of active interface which is the part of the plate containing the actuators that allows the modification of the system's response.

2. THE BLOCH THEOREM APPLIED TO THE ELASTODYNAMIC

In this section, the application of the Floquet-Bloch theorem is presented for piezoelastodynamic problems. Based on the results obtained by Floquet (Floquet,[4] 1883) for monodimensional problems and later rediscovered by Bloch (Bloch,[2] 1928) in multidimensional problems, an original application to bidimensional visco-elasto-dynamic problem has been proposed recently (Collet et al.,[6] 2011) and extended to piezo-elasto-dynamic problem (Collet et al.,[7] 2012).

Further author information: (Send correspondence to Flaviano Tateo)
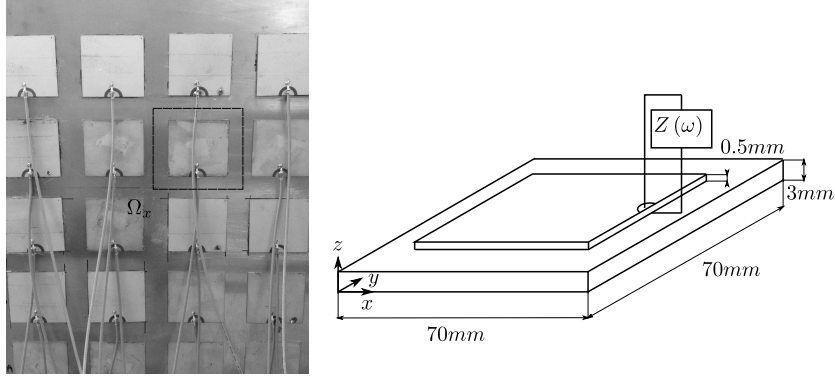Flaviano Tateo: E-mail: flaviano.tateo@femto-st.fr

Figure 1. Actuators periodic lattice and its primitive cell Ω_x.

2.1 The Bloch theorem

The Bloch Theorem stipulates that any function $u(x) \in L^2\left(R^3, C^n\right)$ can be expressed as

$$u(x) = \int_{\Omega_k} e^{ikx} u(x,k) \, dk \tag{1}$$

where the Bloch amplitude $u(x,k)$ is Ω_x-periodic and has the representations

$$u(x,k) = \sum_n u(k+Gn) e^{iGnx} = \frac{\Omega_x}{(2\pi)^3} \sum_n u(x+Rn) e^{ik(x+Rn)} \tag{2}$$

where $u(k)$ stands for the Fourier transform of $u(x)$. It can also be demonstrated that the mean value of the Bloch amplitude is the Fourier amplitude of $u(x)$ for the corresponding wave vector.

Based on that theorem, the expansion functions $v_m(x,k)$ can be defined. They are called the Bloch eigenmodes and can be used to represent the Bloch amplitudes of any solution of periodic problem as

$$u(x,k) = \sum_m u_m(k) v_m(x,k) \tag{3}$$

and at the same time diagonalize the partial derivative operator.

2.2 Application to piezoelastodynamic

Let us consider a piezoelastodynamic problem made of infinite periodic distribution of unitary cell. The harmonic homogeneous dynamical equilibrium of system is driven by the following partial derivative equations

$$\begin{aligned} \rho\ddot{w} - \nabla \cdot \sigma = 0 & \quad \forall x \in \Omega_x \\ -\nabla \cdot D = 0 & \quad \forall x \in \Omega_x \end{aligned} \tag{4}$$

where w is the displacement vector, σ represents the Cauchy stress tensor and D the electric displacement. The linear constitutive material behavior relationships can be written as

$$\begin{aligned} \sigma &= C_E \varepsilon - e^T E \\ D &= e\varepsilon + \epsilon_S E \end{aligned} \tag{5}$$

where $E = -\nabla V$ is the electric field vector (V being the voltage), C_E the elasticity tensor at constant electrical field, ε the Green strain tensor, e^T the piezoelectric coupling tensor, and ϵ_S the dielectric permittivity at constant strain. We add to this set of equilibrium equations an output expression

$$q_{app} = -\int_{S_t} D \cdot n \, dS \tag{6}$$

allowing the introduction of the charge measurement on the piezoelectrics top electrode and hence the dual counterpart of the imposed electrical Dirichlet boundary condition for applying the shunt impedance operator. The equations above are consistent for each kind of material to the extent that null piezoelectric and permittivity tensors can be used when passive materials are considered. All these tensors also depend on the spatial location vector x and are Ω_x periodic. As the problem is 2D infinitely periodic, mechanical boundary conditions are included in the formulation, while electrostatic boundary conditions have to be considered on each cell

$$
\begin{aligned}
V &= 0 & \forall x \in S_b \\
V &= V_{app} & \forall x \in S_t \\
D \cdot n &= 0 & \forall x \in S_l
\end{aligned}
\tag{7}
$$

where S_b is the grounded bottom electrode of the piezoelectric layer, S_t is the top electrode connected to the external shunt, and S_l the lateral electrode. The top electrode applied feedback voltage V depends on the shunt characteristic and on the collected charges q_{app} and can be expressed in the Fourier space by

$$
V_{app} = Z q_{app}
\tag{8}
$$

The proposed formulation is then based on the computation of the Floquet vectors, instead of computing the Floquet propagators commonly used for elastodynamic applications. The full 2D wave dispersion functions can then be obtained, while damping and electrical impedances can clearly be introduced into the piezoelastodynamic operator. The adopted methodology allows the computation of the complete complex map of the dispersion curves incorporating computation of evanescent waves and allowing the introduction of damping and shunt operator if any.

2.3 Numerical computation of the Blochs waves

Replacing the solution expressed in term of the Bloch modes the problem 4 assume the following discretized form:

$$
\left[K\left(Z\left(\omega\right)\right) + \lambda_n\left(\omega, \theta\right) L\left(\theta, Z\left(\omega\right)\right) - \lambda_n^2\left(\omega, \theta\right) H\left(\theta, Z\left(\omega\right)\right) - \omega^2 M \right] u_n\left(\omega, \theta\right) = 0
\tag{9}
$$

where the angular frequency ω is a real parameter corresponding to the harmonic frequency. Wave numbers and Floquet vectors are then computed. This approach allows one to easily take into account the frequency dependency of various system's terms (i.e. damping and electric impedance). An inverse Fourier transformation in the k-space domain can lead us to evaluate the physical wave displacements and energy diffusion operator when the periodic distribution is connected to another system as described in Collet et al.[5] (2009). Another temporal inverse Fourier transformation can furnish a way to access spatio-temporal response for nonhomogeneous initial conditions.

2.4 Computation of the evanescence and damped power flow criteria

One aim of this article is to provide a numerical methodology for optimizing the piezoelectric shunt impedance $Z\left(\omega\right)$ for controlling energy flow into the periodically distributed piezocomposite structure. The first criterion which is considered for describing the capability of the metacomposite for transmitting structural energy is based on the computation of the wave group velocities. Indeed, they indicate how energy is transported into the considered system and allow to distinguish the propagative and evanescent waves.
If a Bloch eigensolution is considered, the associated group velocity vector is given by

$$
C_{g_n} = \nabla_k \omega = \frac{\langle\langle S \rangle\rangle}{\langle\langle e_{tot} \rangle\rangle} = \frac{\langle I \rangle}{\langle E_{tot} \rangle}
\tag{10}
$$

where $\langle\langle . \rangle\rangle$ is the spatial and time average, respectively, on one cell and one period of time; S is the density of energy flow; I is the mean intensity; and e_{tot} and E_{tot} are the total piezomechanical energy and its time average, respectively, on a period. The intensity vector I is expressed as

$$
\langle I_n \rangle = real\left(-\frac{\omega}{2} \int_{\Omega_x} C_E\left(\varepsilon_n + ik\Xi_n\right) \cdot w_n^* \frac{d\Omega}{Vol} \right)
\tag{11}
$$

Plate	Value	Unit
Length	2100	mm
Height	1050	mm
Thickness	3	mm
Mass density	2700	kg/m^3
Young's modulus	$70 \cdot 10^9$	N/m^2
Poisson's ratio	0.33	−
Piezo	Value	Unit
Length	50	mm
Height	50	mm
Thickness	0.5	mm
Mass density	7650	kg/m^3
Poisson's ratio	0.31	−
Dielectic loss	< 0.05	%
Coupling factor	0.51	−

Table 1. Geometry and physical properties of the system.

where * is the complex conjugate, $real$ stands for real part, and Vol the domain volume.

As the spatio-temporal average of the system Lagrangian is null (see Maysenholder,[10] 1994), the total energy average is approximated by only computing the kinetic energy average

$$\langle E_{tot} \rangle = \frac{1}{2Vol} \left(\int_{\Omega_x} \rho \omega^2 w_n \cdot w_n^* d\Omega \right) \tag{12}$$

The group velocity vectors $C_n^g (\omega, \Phi)$ are computed for all wave numbers at each frequency. In order to focus our analysis on only flexural modes (S and SH ones), we introduce an indicator allowing to select them by computing the ratio of kinetic energy average on out-of-plane displacement as

$$Ind\,(n, \omega, \theta) = \frac{\frac{1}{2Vol} \left(\int_{\Omega_x} \rho \omega^2 w_{zn} \cdot w_{zn}^* d\Omega \right)}{\langle E_{tot} \rangle} \tag{13}$$

$w_{zn}(x)$ being the component of vector $w_n(x)$ on z direction. Optimization of the shunt impedance $Z(\omega)$ is based on the minimization of the maximal group velocity collinear to the wave number vector for waves having a ratio of transported flexural kinetic energy greater than the threshold value of 0.8. The criterion can then be written as

$$Crit_1 \,(Z(\omega), \theta) = \max(C_n^g \cdot \Phi) \quad \forall p \in n/Ind\,(n, \omega, \Phi) > 0.8. \tag{14}$$

2.5 Optimization of the flexural energy flow inside the shunted periodic piezocomposite

The considered piezocomposite cell is presented in Figure 1. The supporting plate material is standard aluminum with 0.1% of hysteretic damping ratio, and the piezoelectric material characteristics are given in Table 1. The optimization of the transmission capability of the designed adaptive metacomposite is considered by using $Crit_1$. The objective is to avoid any energy transportation when flexural waves are excited into the periodically distributed shunted piezocomposite cells. The numerical optimization procedure is based on a multidimensional unconstrained nonlinear minimization algorithm (NelderMead). The optimization is done by considering an active/reactive electronic circuit represented by its impedance $Z(\omega)$.

The analysis is initialized with an arbitrary complex value of the shunt impedance. Optimization steps are then proceeded using $Crit_1$ and lead us to obtain frequency-dependent complex impedance for describing the circuit behavior. The real and imaginary parts of the optimal impedance are plotted in Figure 2 for all angles θ. The optimal impedance values almost correspond to a constant negative capacitance in all directions. Equivalent resistances corresponding to the active part of the shunt impedance are negative which indicates that the optimization leads to provide energy to the system for controlling mechanical damping effects introduced by hysteretic terms in the model.
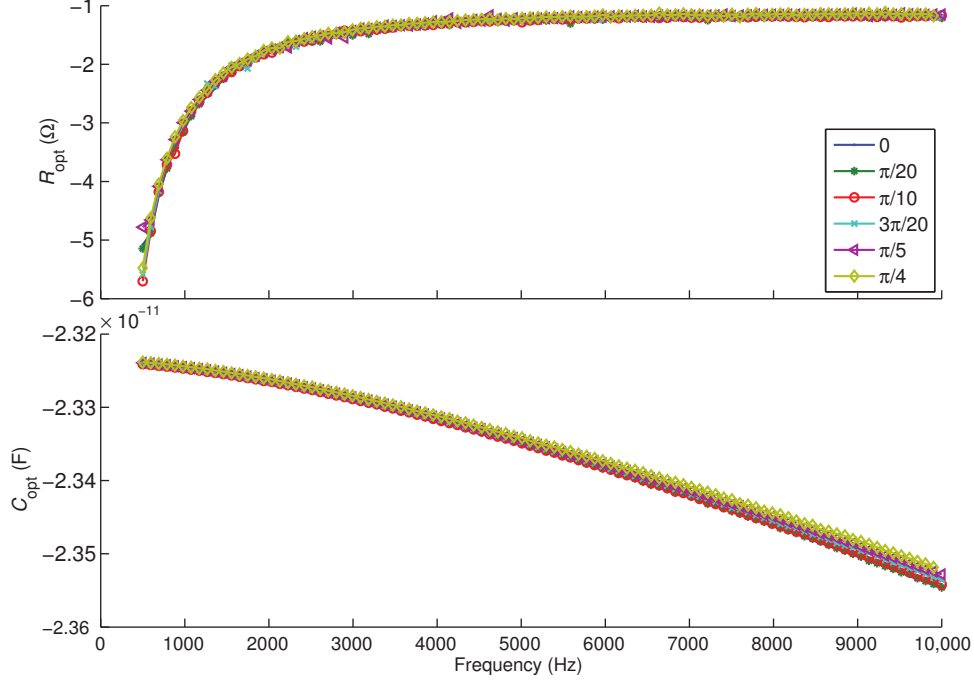
Figure 2. Optimal electric impedance using $Crit_1$.

3. EXPERIMENTAL TEST

This section introduces the design and testing of the smart metacomposite.

3.1 Periodic Lattice design

An aluminum plate with the geometric properties listed in Table 1 is suspended to a rigid frame through metallic wires. The plate is equipped with 75 piezoelectric patches from $PZ26$ series (Ferroperm industries) arranged in a regular 15×5 array. The dimension of the piezoelectric ceramics are listed in Table 1 and are justified by the following assumptions: the plate's dispersion relation of the flexural mode at $5000\ Hz$ has a wavelength of 30 cm. This value imposes a lenght constraint of the piezoceramic in the propagation direction, the best coupling is obtained when the length of the ceramics and the wavelength of the targeted mode respect the ratio of $1/4$. The thickness of the actuator was finally defined considering the restraints of the electric circuit and the nature of the control technique. Different authors argued that the best controlling effect is obtained when the circuit is tuned in correspondence of the biggest ceramic's capacitance value. This property strongly depend on the material properties and the geometry. Once the material properties and the two dimension of the piezoelectric actuator are chosen the only parameter which may be amended is the thickness. Small thicknesses correspond to larger values of the intrinsic capacitance, however, this parameter can not be reduced indefinitely due to the weakening of the piezoelectric ceramic itself. For these reasons a thickness of $0.5\ mm$ was adopted.

3.2 Shunt circuit design

The results derived from the optimization of the external circuit permit to design it in term of real and imaginary part of a general impedance. In Figure 4 is depicted the actual circuit used during the experiment. This circuit contains some passive components such as the resistances R_s, R, R_{tot}, the capacitance C and an active component, namely an operational amplifier that actually allows the circuit to reproduce the intended behavior. This control technique requires a tuning of the synthetic capacitance around the capacitance value of the piezo-electric ceramic, this value is intrinsic and depends upon the material properties and the geometry. The intrinsic capacitance of the piezoelectric ceramic can be easily estimated measuring the capacitance observed by an RLC-meter when the specimen is free of stresses. In the present case the measured value was $52nF$. The actual circuit
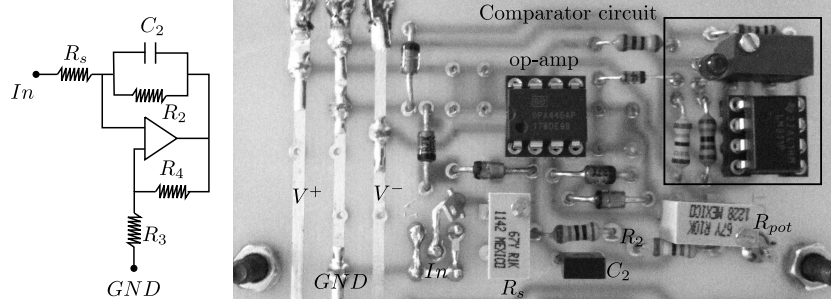
Figure 3. Layout of the electric circuit. Schematic (left), real-life circuit (right).

was tuned varying the position of the potentiometer R_{tot} with small increments. The variation of this parameter determine a variation in the synthetic capacitance according to the formula:

$$C_{eq} = -\alpha C_2 \tag{15}$$

where α is defined as R_4/R_3 and R_{pot} is the resistance of the potentiometer and it represents the sum of R_3 and R_4. The use of the potentiometer simplifies the layout of the circuit because it permits to reproduce the capacitive effect with just one component.

The regulation phase starts setting the synthetic capacitance for very high values and then slowly decreasing it until the desired value is reached. During this phase some problems can occur because of the limitation connected to the nature of the analog circuit. When the external circuit approaches the set-point the system tend to be unstable, an increase of voltage is observed. The operational amplifier is therefore saturated. In order to mitigate this effect the circuit's layout proposed by Beck[1] were modified adding a complementary circuit able to detect this specific instability. Basically a comparator was introduced in correspondence of the op-amp output in order to identify these voltage overloads. This circuit is based on a comparator that measures the differential input between the positive component of the voltage delivered by the operational amplifier in correspondence of the output gate and a reference DC signal from the power supply circuit. Whenever the differential signal results bigger than zero the gate is opened, delivering a current able to illuminate a light emitting diode (LED). This simple solution is very helpful since it allows one to detect this source of instability avoiding the use of the oscilloscope. This feature becomes very useful in this context where a huge number of actuators are involved. For example when several piezoelectric patches are excited a loss of performance can be observed due to the electromechanical coupling occurring between adjacent actuator. In this case, observing the state of the LEDs on the control panel is possible to correctly reset each external circuit.

4. EXPERIMENTAL RESULTS

The experimental procedure involves the measurement of the mobility

$$Y(\omega) = \frac{\dot{w}}{F} \tag{16}$$

where $\dot{w}$ represent the out-of-plane velocity of the controlled plate measured by means of a laser vibrometer and F the shaker's force signal.

In figure 5 the mobility FRF is provided in term of the average of the magnitude using third octave bands, in order to estimate the response reduction of the control system compared with the reference measure made on the same structure without activating the electronic circuit. On the frequency range of interest, it is possible to reduce the transmitted energy of at least 5 dB. However, this is an averaged information, it is possible to obtain, locally, even better results, for example a 15 dB reduction around 2 kHZ. The figure presents two diagrams: the first on the top is related to a measurement made at the excitation point P_1 and the other corresponds to measurements made in the opposite corner of the plate and therefore located downstream with respect the active interface, point P_2. Comparing the two diagrams, an interesting property can be deduced: the plate impedance
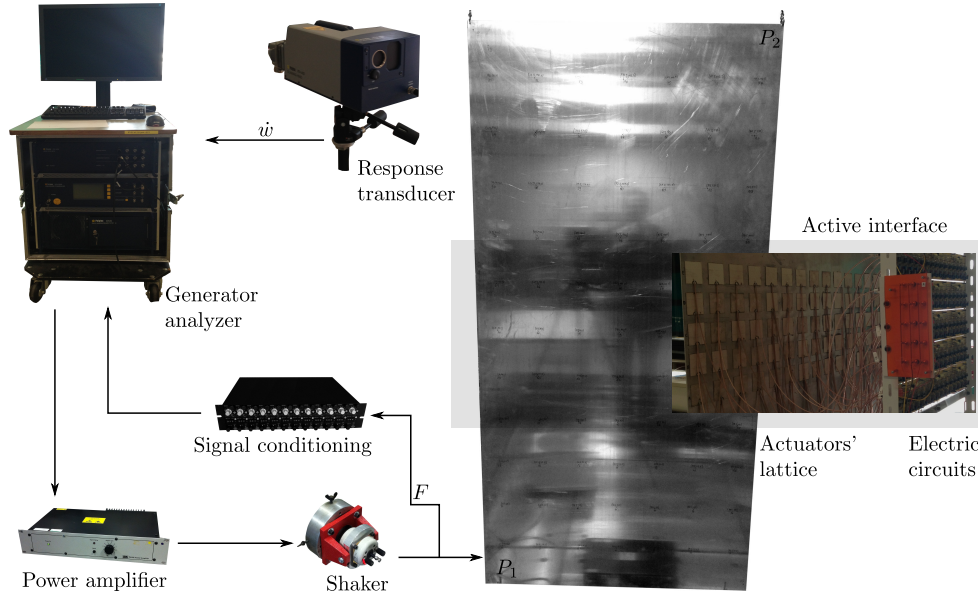
Figure 4. Layout of FRF measurement system.

seen by the excitation is not modified by the control system whereas the part of the plate beyond the active interface acts as the structure would be strongly damped. This effect can be used with profit in case one wants to isolate a source of disturbance.

These results show the effectiveness of the proposed control strategy, it is clear that in the frequency band of $50 - 5000\ Hz$ the control system properly works, reducing the magnitude of the vibrations. However for low frequency values the system seems to be unable to correctly control the underlying structure: the response is amplified during the control phase, this is only due to the deterioration of the measured data, the coherence function shows a poor quality. In order to clarify the system's behavior at low frequency other measurements
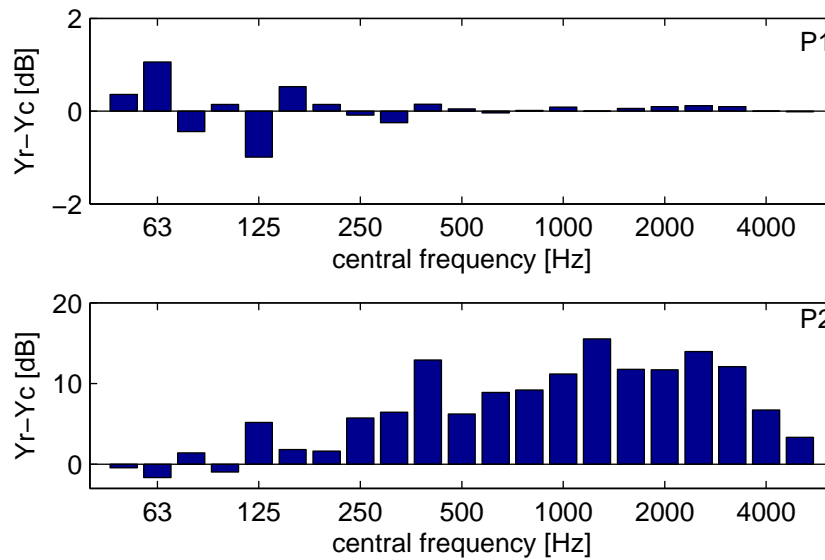

Figure 5. FRF plot comparison between the uncontrolled Y_r and controlled system Y_c expressed in third of octave band.

were performed. In Figure 6 is depicted the plate's frequency response function measured at point P_1 and P_2 of the controlled plate. The mobility function is measured over the frequency range of $0 - 5000\ Hz$, in each row, however, is presented just a small portion of the total FRF in order to point out all the details connected to the dynamics of the system, keeping the best possible values for the coherence function.

In the low frequency range $(0 - 500\ Hz)$ the system cannot be very effective for both positions upstream and downstream, however, beyond $200\ Hz$ the control system is activated, causing an appreciable vibration reduction. On this frequency band the response of the controlled system is constantly smaller than the reference measurement: the control system's main function is to reduce the vibrations adding a certain amount of damping. In Figure 7 a measurement of the plate's velocity distribution is provided. In the top of the image is presented the velocity field of the plate of the reference measurement (control off) against the controlled one in the frequency range where the system is not effective (low frequencies). As a consequence, the control system can not influence the plane and the response level are comparable. The slight modification of the shape of the mode observed can be justified as follows: the controlled plate in this case is experiencing a stiffness properties' modification (frequency shifting). In the active frequency band the response level are decreased in a uniform fashion over the whole region. In this case the wave confinement effect is still present demonstrated by an increase of response level in the portion of the plate behind the active interface delimited by the two horizontal lines.

5. CONCLUSIONS

This article presents a numerical procedure able to compute the damped wave dispersion functions in the whole first Brillouin domain of multidimensional damped piezoelastodynamical wave guides. The method was applied for determining the optimal shunt impedance allowing the minimization of the group velocities of the flexural waves and the damping capability of the distributed system. The proposed methodology can also be used for studying particular dissipation phenomenon such as those induced by complex shunted piezoelectric patches or even foams or complex polymers behaviors.

From the experimental point of view, we showed how it is possible to modify the dynamics of the plate equipped by a series of piezoelectric actuators shunted to negative capacitance circuits and arranged in a periodic fashion. The aim of the project was achieved overcoming several difficulties such as the circuit instability around the set point and the electrical coupling between the different piezoelectric actuators.

These preliminary results are encouraging, however further analysis will be required in order to thoroughly understand the mechanisms related to this control technique. In particular it will be necessary to better match the theoretical results with the experimental measurements.

ACKNOWLEDGMENTS

REFERENCES

[1] Beck B., Cunefare K.A., and Ruzzene M. Broadband vibration suppression assessment of negative impedance shunts. In ASME, editor, *Conference on smart materials, adaptive structures and intelligent systems*, Ellicott City, October 2008.

[2] Bloch F. Über die quantenmechanik der electron in kristallgittern. *Zeitschrift für Physik*, 52:550–600, 1928.

[3] Casadei F., Beck B., Ruzzene M., and Cunefare K.A. Vibration control of plates featuring periodic arrays of hybrid shunted piezoelectric patches. In SPIE, editor, *Conference on smart structures and materials*, San Diego, March 2009.

[4] Floquet G. Sur les équations différentielles linéaires à coefficients périodiques. *Annales Scientifiques de l'École Normale Supérieure*, 12:47–88, 1883.

[5] Collet M., Cunefare K.A., and Ichchou M.N. Wave motion optimization in periodically distributed shunted piezocomposite beam structures. *Journal of Intelligent Material Systems and Structures*, 20:787–808, 2009.

[6] Collet M., Ouisse M., Ruzzene M., and Ichchou M.N. Floquet-bloch decomposition for the computation of dispersion of two-dimensional periodic, damped mechanical systems. *International Journal of Solids and Structures*, 48:2837–2848, 2011.

[7] Collet M., Ouisse M., and Ichchou M.N. Structural energy flow optimization through adaptive shunted piezoelectric metacomposites. *Journal of Intelligent Material Systems and Structures*, 23:1661–1677, 2012.

[8] Hagood N.W. and Von Flotow A. Damping of structural vibrations with piezoelectric materials and passive electrical networks. *Journal of Sound and Vibration*, 146:243–268, 1991.

[9] Reza Moheimani S.O.R. and Fleming A.J. *Piezoelectric transducers for vibration control and damping.* Springer, 2010.

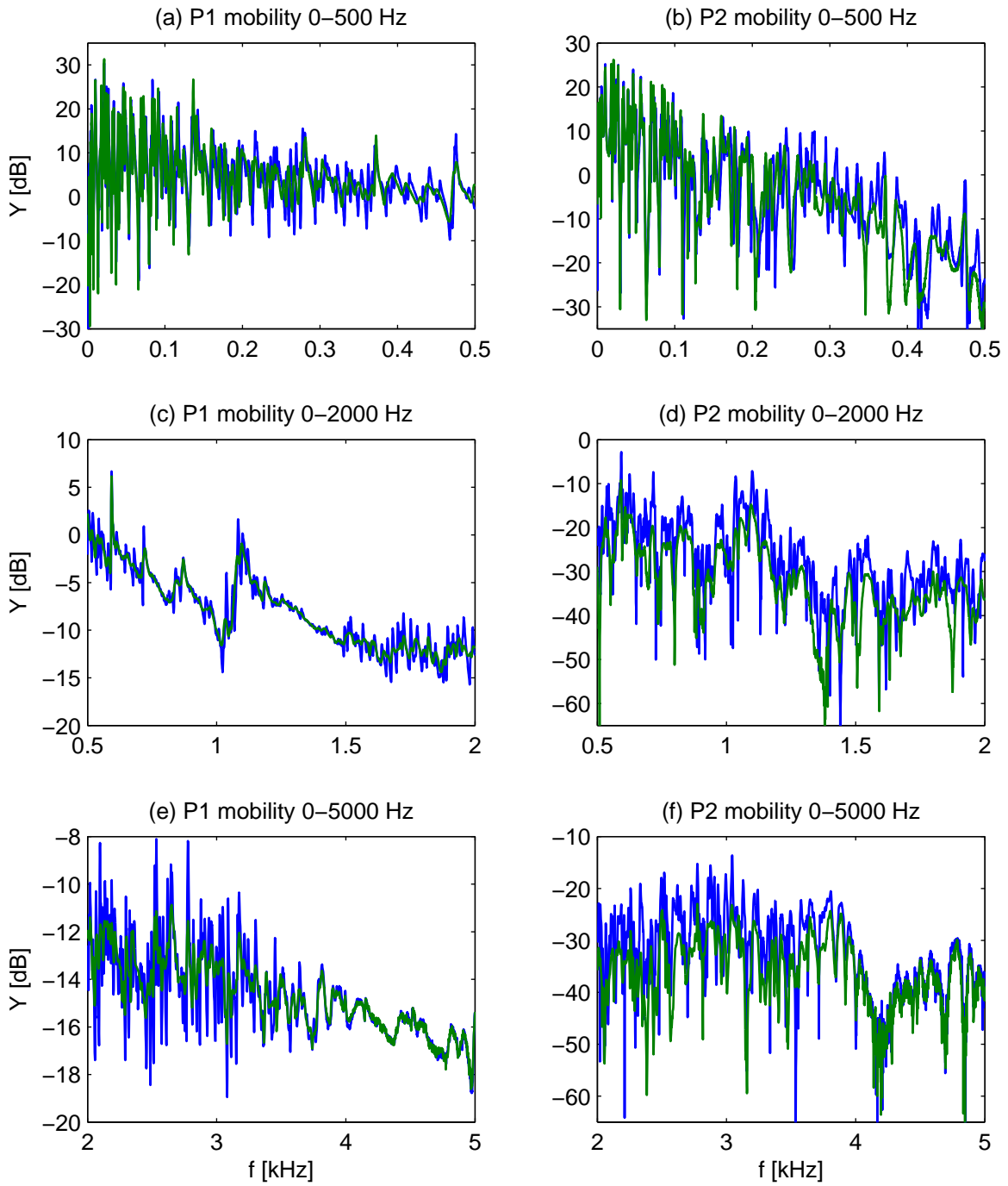[10] Maysenholder W. *Körperschallenergie.* Hirzel, 1994.

Figure 6. FRF plot comparison between the uncontrolled (blue line) and controlled system (green line). P1 measurement (left column), P2 measurement (right column).
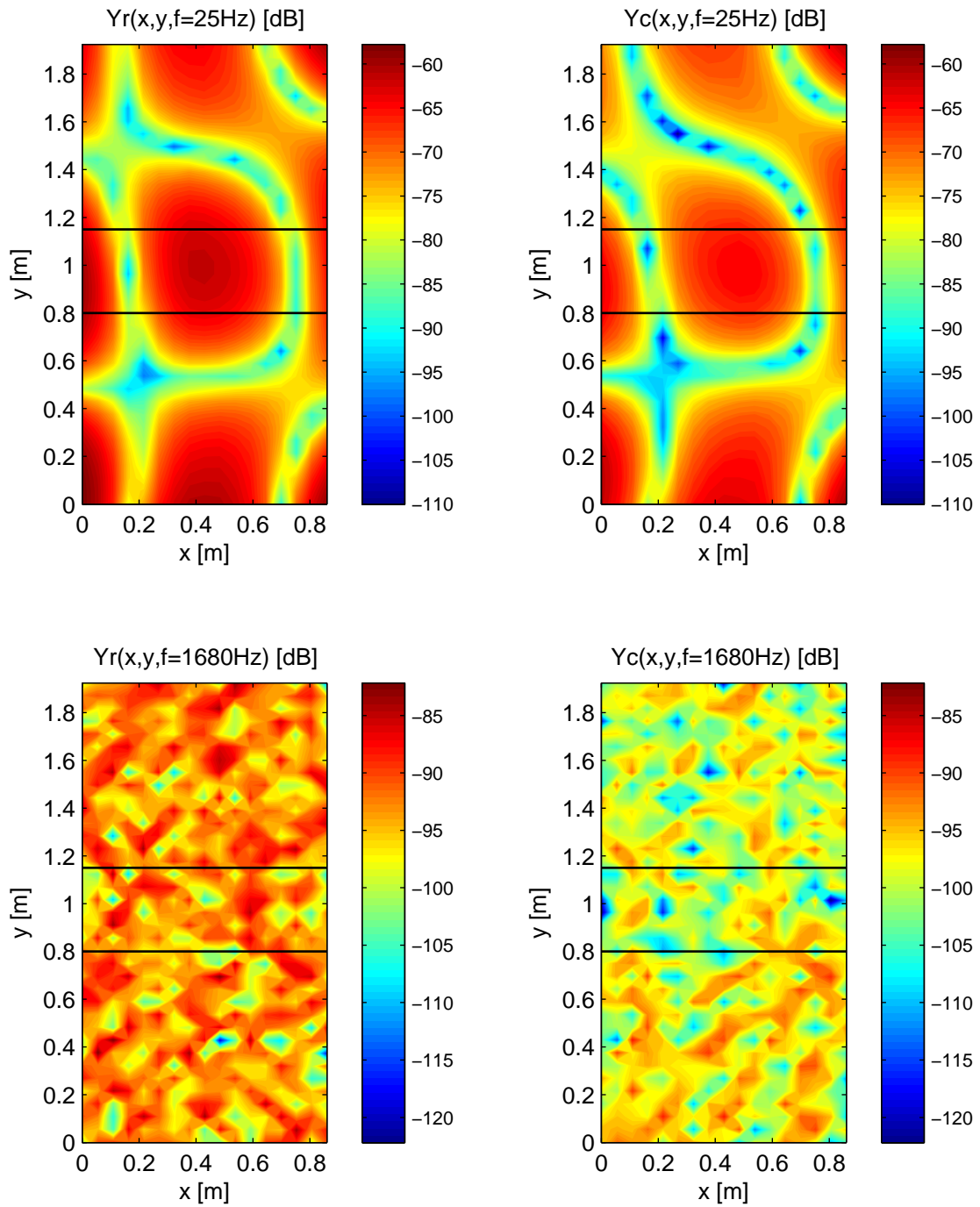
Figure 7. FRF velocity field comparison. Top: inactive region for the control system. Bottom: active region for the control system.